

^{81}Br NQR and ^{119}Sn Mössbauer Study for MSnBr_3 ($\text{M}=\text{Cs}$ and CH_3NH_3)

Koji YAMADA,* Sayuri NOSE, Takako UMEHARA, Tsutomu OKUDA, and Sumio ICHIBA

Department of Chemistry, Faculty of Science, Hiroshima University, Higashisenda-machi, Naka-ku, Hiroshima 730

(Received April 8, 1988)

Successive phase transitions were observed for CsSnBr_3 and $\text{CH}_3\text{NH}_3\text{SnBr}_3$ by means of ^{81}Br NQR and DTA. These compounds are isomorphous with each other and have typical cubic perovskite structures at room temperature. However, with decreasing temperature both compounds showed successive phase transitions and complex ^{81}Br NQR spectra at 77 K. In the case of $\text{CH}_3\text{NH}_3\text{SnBr}_3$, both ^{81}Br NQR and ^{119}Sn Mössbauer spectra changed markedly with decreasing temperature from those at room temperature. These findings suggested a large distortion of the SnBr_6 octahedron from the regular one and were interpreted on the basis of the three-center-four-electron bond model. In relation to these structural changes, a broad-line ^1H NMR experiment on $\text{CH}_3\text{NH}_3\text{SnBr}_3$ was also observed in order to determine the effect of the dynamic properties of the cation.

Trihalostannate anions, SnX_3^- ($\text{X}=\text{Cl}$, Br , and I), in the solid state still provide us with interesting problems, since the anion changes its structure variously with the replacement of the counter cation. Furthermore, drastic changes of the ^{81}Br NQR spectra accompanied by phase transitions have been reported with decreasing temperature.¹⁾ The structural variety of the SnX_3^- anion has been understood on the basis of the stereochemical activity (or nonactivity) of the non-bonding pair of s-electrons.²⁾ In the series of our NQR and Mössbauer studies on SnX_3^- anions, however, the structural variety and phase transitions have been discussed on the basis of the hypervalent character of the central metal.³⁾ In other words, the trans Br-Sn-Br bond is described as a three-center-four-electron (3c-4e) bond.⁴⁾ This bond changes continuously from a symmetric X-Sn-X to an asymmetric $\text{X-Sn}\cdots\text{X}$, as has been observed for the trans Br-Sb-Br bond in $(\text{C}_5\text{H}_5\text{NH})\text{SbBr}_4$.⁵⁾ In this model an inter anionic interaction, such as $\text{X-Sn}\cdots\text{X}$, can also be regarded as an extremely asymmetric case of the 3c-4e bond. According to the crystal structures containing SnX_3^- anions, the tin atom forms regular or distorted octahedron with six nearest-neighbor halogens. Therefore, four structural models shown in Fig. 1 can be systematically understandable in terms of whether

the trans X-Sn-X bond is a symmetric or asymmetric in each of the three orthogonal directions.¹⁾ The appearance of models (B), (C), and (D) can be interpreted as being a result of a displacement of the central metal in the three different directions shown in model (A). The model (A) structure has been reported for CsSnBr_3 ,^{6,7)} model (B) for $\text{KSnF}_3 \cdot (1/2)\text{H}_2\text{O}$,⁸⁾ model (C) for CsSnI_3 ⁹⁾ and $(\text{NH}_4)\text{SnBr}_3 \cdot \text{H}_2\text{O}$,^{1,10)} and model (D) for CsSnCl_3 .¹¹⁾ In our previous paper model (C) anions in $\text{MSnBr}_3 \cdot \text{H}_2\text{O}$ ($\text{M}=\text{K}$ and NH_4) changed their structure with decreasing temperature toward model (D), at which the ^{81}Br NQR frequencies assigned to the basal plane increased enormously.¹⁾

In this paper the structural phase transitions for CsSnBr_3 and $\text{CH}_3\text{NH}_3\text{SnBr}_3$ were studied by means of ^{81}Br NQR, DTA, ^{119}Sn Mössbauer effect, and ^1H NMR. Especially in the CH_3NH_3^+ analogue, the tin environment changed from a regular octahedron at room temperature to a markedly distorted one at 77 K, as was expected from the 3c-4e bond. Furthermore, an interesting problem is the relationship between the 3c-4e bond model and the semimetallic conductivity of the perovskite structure. For the Cs analogue, both experimental and theoretical studies concerning the electric structure have been reported.¹²⁾

Experimental

$\text{CH}_3\text{NH}_3\text{SnBr}_3$ was crystallized as red crystals from ethanol containing stoichiometric amounts of SnBr_2 and $\text{CH}_3\text{NH}_3\text{Br}$. This compound is unstable in air, especially if there exists a trace of hydrobromic acid. CsSnBr_3 was obtained from a melt using a Bridgman furnace. These two compounds were identified to be isomorphous with each other at room temperature using powder X-ray diffraction. The cell constants of the cubic perovskite were determined to be $a=5.808$ and 5.901 Å for Cs and CH_3NH_3 salts, respectively. The former lattice constant agreed well with the value reported previously, $a=5.804$ Å.⁶⁾

$^{79,81}\text{Br}$ NQR was detected with a pulsed spectrometer and was assigned using the quadrupole moment ratio, $Q(^{79}\text{Br})/Q(^{81}\text{Br})=1.1971$. At low temperature, owing to their large line width (ca. 100 KHz), only spin echo signals could be detected using 90° — 180° pulses. ^{119}Sn Mössbauer spectra were recorded by means of a constant acceleration type spec-

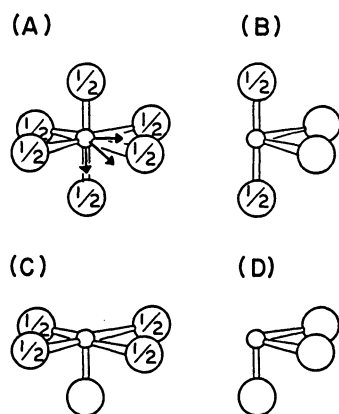


Fig. 1. Structural models for SnX_3^- anion on the basis of octahedral environment around the Sn.

trometer, using $\text{Ca}^{119\text{m}}\text{SnO}_3$ as a gamma-ray source. The velocity was calibrated with Sn and BaSnO_3 .

Results and Discussion

^{81}Br NQR and DTA. Figure 2 shows the temperature dependence of the ^{81}Br NQR frequency for CsSnBr_3 . The phase transition temperatures were determined to be 290 ± 1 and 85 ± 2 K, the former agreeing well with the value reported previously by Scaife et al.¹³⁾ Both transitions were accompanied by a continuous temperature dependence of the NQR frequency and no thermal hysteresis, characteristics of a second-order transition. A preliminary experiment concerning the NQR spin-lattice relaxation times also showed a character of the second-order type phase transition; steep minima in the T_1 vs. temperature curve near the phase-transition temperatures. The intermediate phase II has two NQR lines with intensity ratio 2:1,

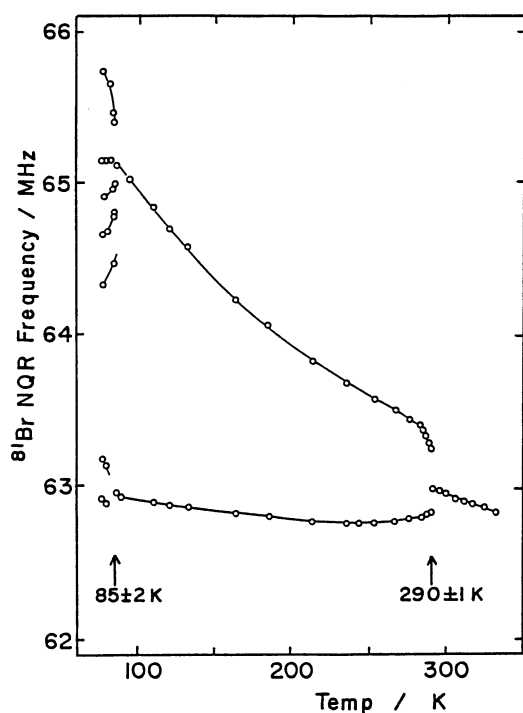


Fig. 2. Temperature dependence of the ^{81}Br NQR frequencies for CsSnBr_3 . Three phases I, II, and III exist between 77 and 330 K from the lowest.

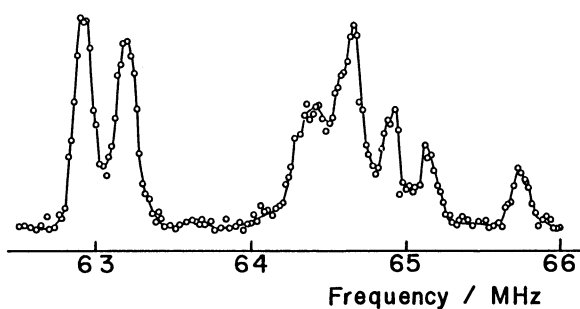


Fig. 3. ^{81}Br NQR spectrum for CsSnBr_3 at 77 K using a spin-echo method.

from the highest, suggesting a tetragonally distortion of the perovskite. As Fig. 3 shows, however, the spectra at 77 K is complicated. At least seven ^{81}Br lines could be detected separately, though the exact number of nonequivalent Br sites could not be determined due to the broad linewidth. However, the distortion of the SnBr_6 octahedra from a regular form is considered to be only slight because of the small splitting of the NQR frequencies. This was also supported by the ^{119}Sn Mössbauer spectrum, which had no quadrupole splitting (as described later).

Figure 4 shows the temperature dependence of the ^{81}Br NQR frequency for $\text{CH}_3\text{NH}_3\text{SnBr}_3$. One ^{81}Br NQR line was observed near 66 MHz at room temperature, as was expected from the cubic perovskite structure. This NQR signal disappeared at 232 K with decreasing temperature and six new lines appeared at about 180 K, as shown in Fig. 4. Because of the wide distribution of the spectra at 77 K, one part of the $^{79,81}\text{Br}$ NQR spec-

Table 1. ^{81}Br NQR Frequencies for MSnBr_3 ($\text{M}=\text{Cs}$ and CH_3NH_3)^{a)}

Compounds	Frequency/MHz	
	77 K	296 K
CsSnBr_3	65.72, 65.13, 64.90, 64.65 64.39, 63.18, 62.92	62.970
$\text{CH}_3\text{NH}_3\text{SnBr}_3$	74.95, 72.83, 71.93 67.15, 65.85, 61.85	65.766

a) Estimated errors ± 0.05 and ± 0.005 MHz at 77 and 296 K, respectively.

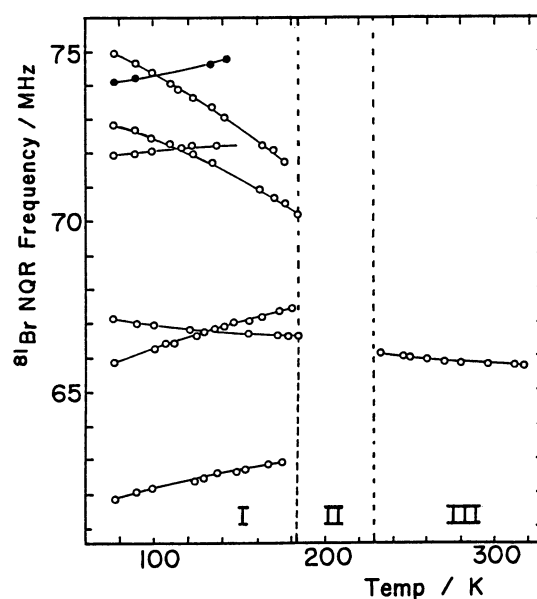


Fig. 4. Temperature dependence of the ^{81}Br NQR frequencies for $\text{CH}_3\text{NH}_3\text{SnBr}_3$. A part of the ^{79}Br NQR line was also observed in the same frequency range because of the wide distribution of the spectrum. Dotted lines show the averaged phase transition temperatures determined by the DTA.

tra overlapped with each other, as shown in Fig. 4. The DTA measurements for this compound are shown in Fig. 5 in the temperature range 160–280 K. Two large peaks corresponding to solid-solid phase transitions appeared with several degrees of hysteresis. Between these two peaks a very small one appeared, though it could not be confirmed by the NQR because of there being no signal in this intermediate phase. Therefore, at least three phases (I, II, and III) exist between 300 and 77 K. Associated with the phase transition between II \leftrightarrow III, the color changed drastically from red to yellow, suggesting a significant structural change. In relation to these successive phase transitions, it is particularly interesting that the splitting of the NQR frequency at 77 K is considerably larger for $\text{CH}_3\text{NH}_3\text{SnBr}_3$ than that expected from the crystal field effect. That is, the highest frequency, about 75 MHz, is comparable to that of a discrete pyramidal SnBr_3^- anion having model (D);¹⁾ the lowest one, about 62 MHz, is lower than that of a room-temperature perovskite structure having model (A). These findings suggest that there are at least two different SnBr_3^- anions having distorted SnBr_6 octahedra (such as model (B), (C), or (D)) in the phase I.

Recently, in the course of this study, similar structural phase transitions from model (A) to (D) were reported for a series of CsGeX_3 ($\text{X}=\text{Cl}, \text{Br}, \text{and I}$)¹⁴⁾ in which the GeX_3^- anions have the same valence electron configuration as that of SnX_3^- . The high-temperature phase of these compounds belongs to a cubic perovskite, so that the trans Br-Ge-Br bond is symmetric. In the low-temperature phase, however, the Ge atom in the halogen octahedral is considerably

displaced from the center of the octahedra along the three-fold axis and the octahedra becomes distorted rhombohedrally. Hence, three trans X-Ge-X bonds become asymmetric X-Ge...X and the anion can also be regarded as an isolated anion. These structural changes are expected for a main-group element having a valence state with an s-electron lone pair, such as Sn(II), Ge(II), As(III), Sb(III), and Te(IV). The nuclear quadrupole resonance of halogens is a useful technique for this problem and drastic NQR frequency shifts have been observed for $\text{MSnBr}_3 \cdot \text{H}_2\text{O}$ ¹⁾ and $(\text{C}_5\text{H}_5\text{NH})\text{SbBr}_4$.⁵⁾

The ^{119}Sn Mössbauer Effect for the MSnBr_3 ($\text{M}=\text{Cs}$ and CH_3NH_3). ^{119}Sn Mössbauer spectra at 93 K are shown in Fig. 6. A quadrupole splitting appears only for $\text{CH}_3\text{NH}_3\text{SnBr}_3$, as was expected from the ^{81}Br NQR. On the other hand, the spectra at 293 K are very weak single Lorentzian, having ca. 1% relative absorption. ^{119}Sn Mössbauer parameters at 293 and 93 K are summarized in Table 2. It is particularly significant that not only the quadrupole splitting but also the isomer shift changed drastically only for the CH_3NH_3^+ analog with decreasing temperature. These results suggest that the symmetry at the Sn site lowered and the s-electron density decreased accompanied by structural phase transitions. This large change of the Mössbauer parameters is reasonable if some structural change

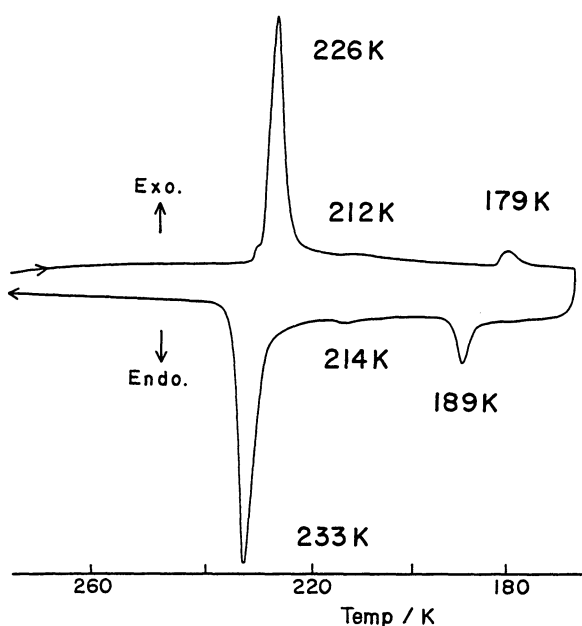


Fig. 5. DTA curve for $\text{CH}_3\text{NH}_3\text{SnBr}_3$ in the temperature range 280–160 K. The transition temperatures, which were determined at the peak positions, show several degrees of hysteresis.

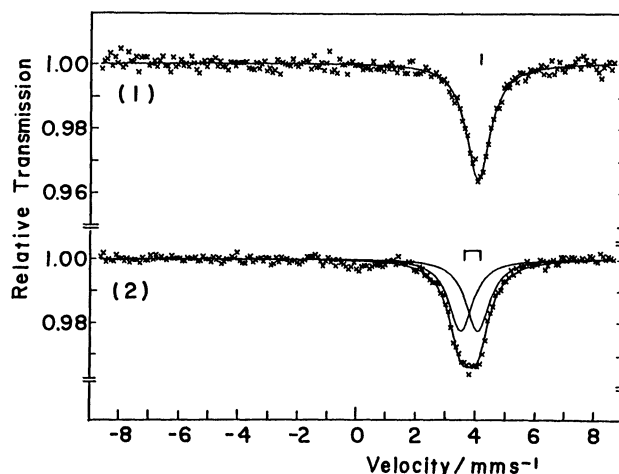


Fig. 6. ^{119}Sn Mössbauer spectra for CsSnBr_3 (1) and $\text{CH}_3\text{NH}_3\text{SnBr}_3$ (2) at 93 K.

Table 2. ^{119}Sn Mössbauer Parameters for MSnBr_3 ($\text{M}=\text{Cs}$ and CH_3NH_3)^{a)}

Compound	Temp K	I.S. mm s^{-1}	Q.S. mm s^{-1}	Line width mm s^{-1}
CsSnBr_3	293	4.00	0	0.84
	93	4.01	0	0.91
	80 ^{b)}	3.98	0	0.84
$\text{CH}_3\text{NH}_3\text{SnBr}_3$	293	3.98	0	1.05
	93	3.81	0.54	0.99

a) Estimated error $\pm 0.03 \text{ m s}^{-1}$. b) Ref. 23.

from model (A) to (D) or (B) takes place. In the case of model (A), the tin atom forms symmetric 3c-4e bonds in three orthogonal directions, so that there is no s-orbital hybridization to the bonds. On the other hand, in the model (D) or (B) structure, the bond angle of the SnBr_3^- anion (Br-Sn-Br) becomes slightly larger than 90 degrees and, hence, a hybridization of the s-orbital to the p-orbitals takes place.¹⁵⁾ Thus, the smaller isomer shifts at 93 K than 293 K can be attributed to a decrease in the s-electron density due to a hybridization of the s-orbital to the pure p-orbital bonding.

^1H NMR for $\text{CH}_3\text{NH}_3\text{SnBr}_3$. In order to examine the relationship between these phase transitions and the dynamical property of the cation, the ^1H NMR was observed as a function of temperature (Fig. 7). The calculated second moments in phases I and III were almost constant and were 8 ± 0.5 and $0.5 \pm 0.1 \text{ G}^2$ ($1 \text{ G} = 10^{-4} \text{ T}$), respectively. According to the previous ^1H NMR studies containing the same cation, the second moment of about $7\text{--}8 \text{ G}^2$ corresponds to the reorientational motion of the cation around its C_3 axis.¹⁶⁻¹⁹⁾ The second moment of about 0.5 G^2 corresponds to an interionic contribution, indicating that an overall rotation of the cation takes place at a rate higher than $\text{ca. } 10^5 \text{ s}^{-1}$. These phase transitions take place at almost the same temperature at which the 2nd moment changed stepwise. These results suggest that the phase transitions are largely affected by the dynamical properties of the CH_3NH_3^+ cation. Many structural phase transitions containing the CH_3NH_3^+ cation have been reported, partly because of a change in the effective volume and partly because of a breakdown of the

hydrogen-bonding networks.²⁰⁻²²⁾ In this case, it is particularly noteworthy that the structure and the bonding of the anion are also affected associated with these phase transitions due to the nature of the 3c-4e bond.

References

- 1) K. Yamada, T. Hayashi, T. Umehara, T. Okuda, and S. Ichiba, *Bull. Chem. Soc. Jpn.*, **60**, 4203 (1987).
- 2) N. N. Greenwood and A. Earnshaw, "Chemistry of the elements," Pergamon Press (1984), p. 439.
- 3) T. A. Albright, J. K. Burdett, and M. H. Whangbo, "Orbital Interactions in Chemistry," John Wiley & Sons, New York (1985), p. 258.
- 4) G. C. Pimentel, *J. Chem. Phys.*, **19**, 446 (1951).
- 5) T. Okuda, K. Yamada, H. Ishihara, M. Hiura, S. Gima, and H. Negita, *J. Chem. Soc., Chem. Commun.*, **1981**, 979.
- 6) J. Barrett, S. R. A. Bird, J. D. Donaldson, and J. Silver, *J. Chem. Soc. A*, **1971**, 3105.
- 7) J. D. Donaldson, J. Silver, S. Hadjiminolis, and S. D. Poss, *J. Chem. Soc., Dalton Trans.*, **1974**, 1500.
- 8) V. G. Bergerhoff, L. Goost, and E. Shultze-Rhonhof, *Acta Crystallogr., Sect. B*, **24**, 803 (1968).
- 9) P. Mauersberger and F. Huber, *Acta Crystallogr., Sect. B*, **36**, 683 (1980).
- 10) J. Andersson, *Acta Chem. Scand., Ser. A*, **30**, 229 (1976).
- 11) F. R. Poulsen and S. E. Rasumussen, *Acta Chem. Scand.*, **24**, 150 (1970).
- 12) D. E. Parry, M. J. Tricker, and J. D. Donaldson, *J. Solid State Chem.*, **28**, 401 (1979).
- 13) D. E. Scaife, P. F. Weller, and W. G. Fisher, *J. Solid State Chem.*, **9**, 308 (1974).
- 14) G. Thiele, H. W. Rotter, and K. D. Schmidt, *Z. Anorg. Allg. Chem.*, **545**, 148 (1987).
- 15) M. J. Tricker and J. D. Donaldson, *Inorg. Chem. Acta*, **31**, L445 (1978).
- 16) R. Ikeda, Y. Kume, and D. Nakamura, *J. Magn. Reson.*, **24**, 9 (1976).
- 17) Y. Kume, R. Ikeda, and D. Nakamura, *J. Phys. Chem.*, **82**, 1926 (1978).
- 18) R. Jakubas, Z. Czaplá, Z. Galewski, L. Sobczyk, O. J. Zogal, and T. Lis, *Phys. Status Solid A*, **93**, 449 (1986).
- 19) Y. Kume, R. Ikeda, and D. Nakamura, *J. Magn. Reson.*, **20**, 276 (1975).
- 20) F. Milia, *Solid State Commun.*, **51**, 625 (1984).
- 21) H. Fuess, M. Korfer, H. Arend, and R. Kind, *Solid State Commun.*, **56**, 137 (1985).
- 22) H. Ishida, R. Ikeda, and D. Nakamura, *J. Chem. Soc., Faraday Trans. 2*, **81**, 963 (1985).
- 23) J. D. Donaldson, R. M. A. Grimsey, and S. J. Clark, *J. Phys. (Paris)*, **40**, C2-289 (1979).

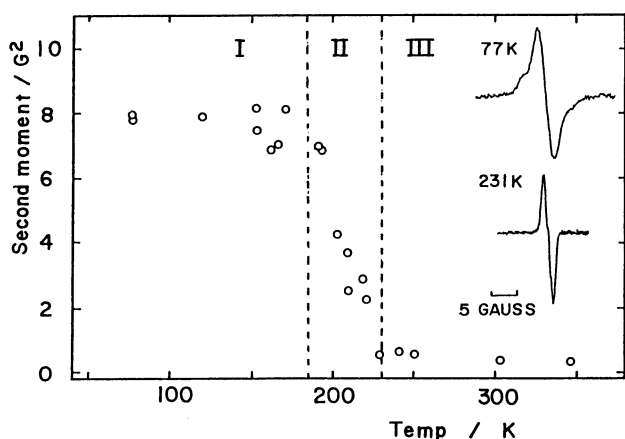


Fig. 7. Temperature dependence of the ^1H NMR second moment for $\text{CH}_3\text{NH}_3\text{SnBr}_3$.